Polymers **2015**, *7*, 1427-1443; doi:10.3390/polym7081427

OPEN ACCESS

polymers

ISSN 2073-4360

www.mdpi.com/journal/polymers

Article

Stable Poly(methacrylic acid) Brush Decorated Silica Nano-Particles by ARGET ATRP for Bioconjugation

Marcello Iacono [1,2] and Andreas Heise [1,3,*]

[1] School of Chemical Sciences, Dublin City University, Dublin 9, Ireland; E-Mail: marcello_iacono@hotmail.com

[2] Biomedical Diagnostics Institute, Dublin City University, Dublin 9, Ireland

[3] School of Pharmacy, Royal College of Surgeons in Ireland, Dublin 2, Ireland

* Author to whom correspondence should be addressed; E-Mail: andreas.heise@dcu.ie; Tel.: +353-1-700-6709; Fax: +353-1-700-5503.

Academic Editor: Walter Remo Caseri

Received: 15 June 2015 / Accepted: 28 July 2015 / Published: 6 August 2015

Abstract: The synthesis of polymer brush decorated silica nano-particles is demonstrated by activator regeneration by electron transfer atom transfer radical polymerization (ARGET ATRP) grafting of poly(*tert*-butyl methacrylate). ATRP initiator decorated silica nano-particles were obtained using a novel trimethylsiloxane derivatised ATRP initiator obtained by click chemistry. Comparison of de-grafted polymers with polymer obtained from a sacrificial initiator demonstrated good agreement up to 55% monomer conversion. Subsequent mild deprotection of the *tert*-butyl ester groups using phosphoric acid yielded highly colloidal and pH stable hydrophilic nano-particles comprising approximately 50% methacrylic acid groups. The successful bio-conjugation was achieved by immobilization of Horseradish Peroxidase to the polymer brush decorated nano-particles and the enzyme activity demonstrated in a conversion of *o*-phenylene diamine dihydrochloride assay.

Keywords: silica nano-particles; polymer brushes; ARGET ATRP; poly(methacrylic acid); bio-conjugation; enzyme immobilization

---

1. Introduction

The advent of nano-technology and more recently nano-medicine has increased the demand for well-defined nano-particles (NPs) for example in areas such as diagnostics, drug delivery, bio-separation among others [1–6]. Silica nano-particles (Si-NPs) is among the most widely applied class of nano-particles owing to their well-documented synthetic accessibility by the base or acid catalyzed condensation of low molecular weight silicates. This process is known as the Stöber synthesis (and variations thereof) allows the synthesis of Si-NPs ranging from 15 to 800 nm [7,8] with good size control and, if desired, the incorporation of dyes or active molecules [9]. An increasingly important aspect in the design of nano-particles is their surface functionalization to facilitate interaction with the environment, the conjugation of active (bio)-molecules or simply to enhance their colloidal stability. Very useful in that respect are polymer brushes, *i.e.*, functional polymers attached to the nanoparticle surface, due to their high polymer segment density [10,11]. We are interested in the decoration of Si-NPs with poly(methacrylic acid) (PMAA) or poly(acrylic acid) (PAA) as they can easily be conjugated with biomolecules by conventional coupling chemistry [12]. Moreover, the hydrophilic nature of these brushes stabilizes the nano-particle suspension in aqueous media thereby preventing particle aggregation and ensuring extended shelf life [13].

The grafting of polymer chains from the surface of the NP is the most widely used methodology to achieve polymer brush decorated silica nano-particles. Controlled radical polymerization techniques such as atom transfer radical polymerization (ATRP) are particularly useful in that respect as they permit the engineering of polymer brushes of defined length, density, and composition so as to modulate the surface functionality and properties of the NP [14–20]. Although ATRP has been extensively used for the polymer decoration of various surfaces including few examples of PAA and PMAA, it has the drawback of high copper catalyst concentrations. While the catalyst can be removed when micro or macroscopic substrates are used (e.g., silicon wafers), removal of the catalyst from NP is challenging. This drawback can be overcome by activator regeneration by electron transfer (ARGET) ATRP [21–23]. In ARGET ATRP the amount of copper catalyst is significantly reduced by a strategy that employs a reducing agent to *in situ* regenerate the active Cu(I) species. This technique has successfully been employed from surfaces [12,24–28] but to the best of our knowledge there are only very few reports of ARGET ATRP from Si-NP [29,30].

Here we report for the first time the synthesis of PMAA decorated Si-NP by surface initiated ARGET ATRP of *tert*-butylmetharylate (*t*-BMA). Subsequent mild deprotection of the poly(tert-butylmetharylate) (PBMA) yielded hydrophilic PAA decorated Si-NP with high colloidal stability. The feasibility of these nano-particles as a platform for bio-conjugation was shown by the immobilization of Horseradish Peroxidase (HRP).

2. Experimental Section

2.1. Chemicals

All chemicals were obtained from Sigma Aldrich (Dublin, Ireland) and used as received unless otherwise noted. Triphenylphosphine and $CuBr_2$ were obtained from Acros (Geel, Belgium). 1-Ethyl-3-[3-dimethylaminopropyl] carbodiimid and *N*-hydroxysulfosuccinimide were obtained from

Thermo Fisher (Dublin, Ireland). $Cu(PPh_3)_3Br$ was synthesized according to a literature procedure [31]. Peroxidase from horseradish Type VI, essentially salt-free, lyophilized powder, 250–330 units/mg solid (using pyrogallol), *o*-Phenylenediamine tablet (20 mg substrate per tablet), hydrogen peroxide solution (30 wt% in H_2O), 1 M H_2SO_4 were obtained from Sigma Aldrich.

2.2. Methods

^1H and ^{13}C nuclear magnetic resonance (NMR) spectra were recorded at room temperature on a Bruker Avance 400 (400MHz, Bruker, Coventry, UK) and a Bruker Avance Ultrashield 600 (600 MHz, Bruker, Coventry, UK). $CDCl_3$ was used as a solvent and the signals were referred to the signal of residual protonated solvent signals. Thermo-gravimetric analyses (TGA) were performed on a TGA Q50 (TA Instruments, New Castle, PA, USA) from TA Instruments using a temperature ramp from 20 to 800 °C at 20°C/min. under nitrogen atmosphere. All samples were carefully dried before measurement (3 days at 0.1 mbar at RT).

A Perkin-Elmer Spectrum 100 (Perkin-Elmer, Waltham, MA, USA) was used for collecting attenuated total reflectance Fourier transform infrared (ATR-FTIR) spectra in the spectral region of 650–4000 cm^{-1}. The spectra were obtained from four scans with a resolution of 2 cm^{-1}. A background measurement was taken before the sample was loaded onto the ATR unit for measurements. To measure melting points a Gallenkamp melting point apparatus (Gallenkamp, London, UK) has been used. Molecular weights of polymer were characterized by gel permeation chromatography performed on an Agilent 1200 series (Agilent Technologies, Santa Clara, CA, USA) equipped with two PL Gel 5 micrometer Mixed-C 300 × 7.5 mm^2 columns at 40 °C and a differential refractive index (DRI) detector. Tetrahydrofuran (THF) was used as an eluent at a flow rate of 1 mL min^{-1}. Molecular weights were calculated based on poly(methyl methacrylate) standards. TEM images were obtained using a TITAN microscope (FEI, Hillsboro, TX, USA) at Trinity College Dublin CRANN (at an accelerating voltage of 200 kV) for samples deposited on carbon-coated (400 mesh) copper grids. The preparation of samples for transmission electron microscopy (TEM) analysis involved depositing a drop (15 mL) of the nanoparticle suspension in toluene of water onto the grids and allowing the solvent to evaporate prior to imaging. The dynamic light scattering (DLS) experiments of peptide grafted nano-particles in different pH solutions were performed at 25 °C on a ZetasizerNano ZS particle analyzer (Malvern Instruments, Worcestershire, UK) using a detection angle of 173 degree and a 4 mW He–Ne laser operating at a wavelength of 633 nm. Perkin-Elmer Lambda 900 spectrometer (Perkin-Elmer, Waltham, MA, USA) was used for HRP colorimetric tests.

Prop-2-ynyl 2-bromoisobutyrate (V) [32]: A clean round bottom flask (previously dried 1 night in the oven at 140 °C) containing 100 mL of anhydrous ether was cooled to 0 °C using an ice/water bath. The solvent was purged 10 min with N_2 before the addition of 2-bromoisobutryl bromide (20.0 g, 87 mmol) and pyridine (8.3 g, 105 mmol). After 2–3 min. the suspension turned yellow. The mixture was stirred for 5 min. before the drop wise addition of propargyl alcohol (5.87 g, 105 mmol) dissolved in 50 mL of anhydrous ether over a period of 30 min after which the suspension turned white. The flask was then removed from the ice bath and the reaction was allowed to proceed at room temperature for 24 h. The reaction mixture was then washed with 100 mL of 1 M HCl, 100 mL of 1 M NaOH, and 100 mL of brine, and then dried over anhydrous $MgSO_4$. The solvent was removed by rotary evaporation at 35 °C and 0.1 mbar for 1 h

and the alkyne group containing ATRP initiators was obtained as a white solid (yield: 89%). ^{1}H NMR (600 MHz, $CDCl_3$, δ): 4.78 (d, 2H, C*H*$_2$O), 2.55 (t, 1H, C–C*H*) and 1.96 (s, 6H, (C*H*$_3$)$_2$C).

3-Azidopropyltrimethoxysilane (VI) [33]: To a 250 mL round bottom flask, 3-chloropropyltrimethoxysilane **III**, (6 mL, 6.80 g, 32 mmol), sodium azide **IV** (4.2 g, 64 mmol), and *N*,*N*-dimethylformamide (DMF) (40 mL) were added. The reaction mixture was stirred at 100 °C for 24 h. After cooling to room temperature, the mixture was filtered and the filtrate concentrated under reduced pressure by rotary evaporation at 35 °C, 0.1 mbar for 2 h to yield a yellow liquid as product (yield: 3.1 g, 95%). ^{1}H NMR (600 MHz, $CDCl_3$, δ): 3.57 (s, 9H, O–C*H*$_3$), 3.27 (dt, J = 2.7 Hz, 2H, N$_3$–C*H*$_2$), 1.71 (m, 2H, C*H*$_2$), 0.71 (m, 2H, Si-C*H*$_2$).

1-((3-Trimethoxysilyl)propyl))-4-(ylmethyl 2-brono-2-methylpropanate)-1,2,3-triazole (VII): In a round bottom flask 1.2 mol equivalents prop-2-ynyl 2-bromoisobutyrate, 1 mol equivalents 3-azidopropyl trimethoxysilane and 0.5 mol% catalyst $Cu(PPh_3)_3Br$ in DMF are stirred for 24 h at room temperature. After centrifugation and removal of the solvent in a rotary evaporator the product was obtained without further purification as a dark orange oil (density measured at RT is 1.45 g/mL) and stored under N_2 at 4 °C (yield: 78%). ^{1}H NMR ($CDCl_3$, δ): 0.52 (m, 2H, –C*H*$_2$–), 1.91 (s, 8H (6 + 2), (C*H*$_3$)$_2$C) and –C*H*$_2$–), 3.57 (s, 9H, O–C*H*$_3$), 4.32 (m, 2H, –C*H*$_2$–), 5.25 (m, 2H, –C*H*$_2$–O), 8.20 (s, 1H, triazolic C(5) proton). ^{13}C NMR (600 MHz, DEPT, $CDCl_3$, δ) 5.80 (–*C*H$_2$–), 23.70 (–*C*H$_2$–), 30.02 (–*C*H$_3$), 49.90 (–*C*H$_3$), 51.70 (–*C*H$_2$–), 59.10 (–*C*H$_2$–), 124.35 (*C*–H) (^{13}C NMR DEPT assignments confirmed by Heteronuclear Multiple Bond Correlation (HMQC) NMR ^{1}H-^{13}C correlation spectrum).

2.3. Synthesis of Si-NP (Diameter 200 nm)

To prepare a 1 L alcosol batch with Si-NP 200 nm in diameter, 406.5 g of a 7 M solution of ammonia in MeOH are weighed and mixed with water (162.4 g) and TEOS (58.35 g). Finally, 247.3 mL of EtOH were added. The system was left overnight at room temperature. Subsequently the particles were recovered by successive centrifugations/decanted re-suspension cycles in ethanol, acetone and THF.

2.4. Decoration of Silica Nano-Particles with ATRP Initiator VII

The concentration of NP in the decoration suspension can be up to 1 g per 40 mL of solvents (for nano-particles up to 200 nm or less for smaller diameters). The system must be perfectly homogenous and mono-disperse and for this reason a 2 mL properly diluted aliquot of the system at room temperature should be analyzed by DLS at this stage. The acidic (acetic acid, 0.027%, *v*/*v*) suspension in THF of the bare Si-NP is gently stirred for 2 h at 35–40 °C. Then, 2% *v*/*v* of initiator (diluted in 5 mL of THF) is added drop-wise during 5 min under stirring and the system is refluxed under static N_2 flow overnight. As a final step the washed decorated NP are re-suspend in a minimum amount of THF and left overnight under a very gentle flow of N_2 to complete the formation of silanol bonds. The final powder is stored as stock solution in anisole.

2.5. Grafting of Tert-Butyl Methacrylate from ATRP Initiator Decorated Silica Nano-Particles

To a 22.5 mL glass vial (cleaned with acetone and dried by flushing N_2 for 5 min) 100 mg initiator decorated Si-NP were added as an anisole stock suspension (5 mL of 1 g/mL suspension). Then a stirring

bar and 15 mL of *tert*-butyl methacrylate (92.3 mmol) were added. Under magnetic stirring, the sacrificial initiator is added (methyl 2-bromopropionate, 32.80 μL, 0.294 mmol). $CuCl_2$ (0.710 mg, 0.0053 mmol) and TPMA ligand (6.50 mg, 0.0224 mmol) are then added. The vial is then sealed with a rubber septum, purged with nitrogen for several minutes and the reducing agent is added under stirring (tin (II) 2-ethylhexanoate, 109 μL, 0.337 mmol). Note that the removal of oxygen by purging is not required in ARGET ATRP but accelerates the initiation process. The system is left at 60 °C for 4.5 h. The work up is based on six centrifugation steps at 9000 rpm (7890 Relative Centrifugal Force, RCF) for 20 min using toluene to wash the decanted particles (in each re-suspension of the decanted particles 5 min of ultra-sonication is applied). The last steps are three washings in THF and the re-suspended system in THF is left under a mild steam of N_2 overnight at room temperature after which a brownish powder (118 mg) was recovered.

2.6. Reaction Kinetics and Degrafting of Polymer from Si-NP

In order to define the kinetic of the polymer growth, a known amount of DMF was added as an internal (and not reactive) NMR standard. Aliquots of the reaction mixture were withdrawn at time intervals with of a N_2 purged syringe. The samples were immediately exposed to air and cooled to stop the polymerization. After centrifugation, the supernatant was analyzed by ^{1}H-NMR, while the solid Si-NP (properly dried and washed) were treated with HF to de-graft the polymer from the surface. In a 25 mL flat bottom teflon vial, 2.5 mL of hydrofluoric acid solution (48% in H_2O *w*/*w*) was added to 50 mg of brush decorated Si-NP previously suspended in a mixture 1:10 (*v*/*v*) of 0.1 M HCl/THF and stirred at no more than 100 rpm overnight to ensure complete dissolution. The reaction mixture was then added to a polyethylene centrifuge tube the de-grafted polymer was precipitated by adding 10 mL de-ionized water followed by centrifugation at 9000 rpm for 30 min. Traces of HF were then removed by dissolving de-grafted material in 0.5 mL THF and the polymer re-precipitated in 5 mL deionized water. The product was then centrifuged at 6000 rpm for 10 min and five repetitive washings and centrifugations were done with fresh deionized water. The free polymer was dried in a vacuum oven at 40 °C to remove traces of water up to a constant mass.

2.7. Deprotection of Poly(tert-Butyl Methacrylate) Grafted Si-NP

In a typical experiment, aqueous phosphoric acid (85 wt%) was added to a suspension of the brush Si-NP in THF typically with 1 mL of solvent per g of brush and 15 equivalents of aqueous phosphoric acid (85 wt%). The mixture was stirred at room temperature for 12 h (this time refers to the system obtained at 75% monomer conversion). For the workup water was added to dilute the reaction mixture, and concentrated sodium hydroxide solution was added to adjust the pH to 7–8. Final centrifugation steps are repeated up to pH neutrality of the supernatant.

2.8. Bioconjugation with HRP

A 10 mg/mL brush PMAA silica nano-particle suspension in 0.1 M MES (2-morpholino ethanesulfonic acid), 0.5 M NaCl, pH 6.0 buffer was reacted with 1-ethyl-3-(3-dimethyl aminopropyl) carbodiimide (2 mM) and *N*-hydroxysulfosuccinimide (5 mM) at room temperature during 15 min. Then, after fast

centrifugation (2 min) the nano-particles were washed with 0.1 M sodium phosphate, 0.15 M NaCl, pH 7.2–7.5 two times. After decanting the liquid, the solid was diluted in 10 mL of 0.1 M sodium phosphate, 0.15 M NaCl, pH 7.2–7.5 and 5 times 1 mL aliquots are centrifuged. These five samples of activated silica nano-particles are re-dissolved in 930, 940, 950, 960, 970 μL of sodium phosphate buffer. The entire process should be carried as quickly as possible (here 8 min) and at room temperature. Then, aliquots of a freshly prepared solution of Peroxidase from horseradish (HRP) in 0.1 M sodium phosphate, 0.15 M NaCl, pH 7.2–7.5 at 1 mg/mL in HRP are transferred in the activated NP suspension. In particular, five aliquots of 70, 60, 50, 40 and 30 μL of the HRP solution at 1 mg/mL were added to the 1 mg/mL activated nano-particles suspension to obtain 5 times 1 mL samples with the same concentrations of nano-particles (1 mg) and different amounts of HRP. The bio-conjugation reaction was complete within 2 h at room temperature. The work up was made by centrifugation and two washing/re-suspension steps in phosphate-buffered saline (PBS) buffer (centrifugation cycles at 6860 RCF at 8500 rpm for 3 min). The final samples were stored in 0.1 M PBS buffer at pH = 6.0 at 4 °C for no more than two weeks, based on the stability of the HRP at concentrations of 1 mg of bio-conjugated nano-particles per mL of buffer. The specific tests here were carried out with 1 day to 2 weeks old bio-conjugated NP with no difference in the final colorimetric test.

2.9. Colorimetric Test

A buffer solution was prepared with 10.19 g of anhydrous citric acid, 30.90 g of $Na_2HPO_4 \cdot 12H_2O$ (or, as an alternative, 14.60 g of Na_2HPO_4) at pH = 5 in 1 L of ultrapure water (18 MW/cm). A 20 mg tablet of *o*-phenylene diamine is dissolved in 50 mL of this buffer and left in the dark. Immediately before the colorimetric test, 20 μL of H_2O_2 (30% *v*/*v*) were added. To each aliquot of bio-conjugate at 1 mg/mL, 0.1 mL of this buffer is added. The system is left in the dark at room temperature during 2 h then 25 μL 1 M H_2SO_4 are added to stop the reaction. The system is then measured in a UV spectrophotometer at $l_{MAX} \approx 441$ nm.

3. Results and Discussion

The synthesis of the brush decorated Si-NP include the surface decoration of the bare nanoparticles with an ATRP initiator, the polymerization of *t*-BMA and a final deprotection step of the poly(*t*-BMA) to form the PMAA brush. The Si-NPs used in this work have an average diameter of 200 nm (PDI = 0.014) and were obtained by a classical Stöber synthesis from tetraethoxyorthosilicate (TEOS) [7]. The introduction of the initiator groups to the NP surface was achieved using a silane coupling agent employing "click" chemistry [34,35]. Using the click approach, an azido-modified silane moiety **VI** was readily "clicked" on an alkyne-functional bromoester **V** (Scheme 1). The initiator **VII** was obtained as a dark orange oil. The NMR spectra (Figure S1) of **VII** confirm the successful synthesis, in particular the singlet **d** at 8.20 ppm in the aromatic region of the ^{1}H NMR spectrum due to the formation of the 1,2,3-triazolic ring [36]. This multi-step reaction is easy to perform, produces high yields and is robust so that sufficient amounts of initiator can be synthesized. While only applied for the synthesis of an ATRP initiator functional silane coupling agent, this strategy would allow preparing initiators for a number of similar techniques just by changing the final active initiator group for the desired polymerization.

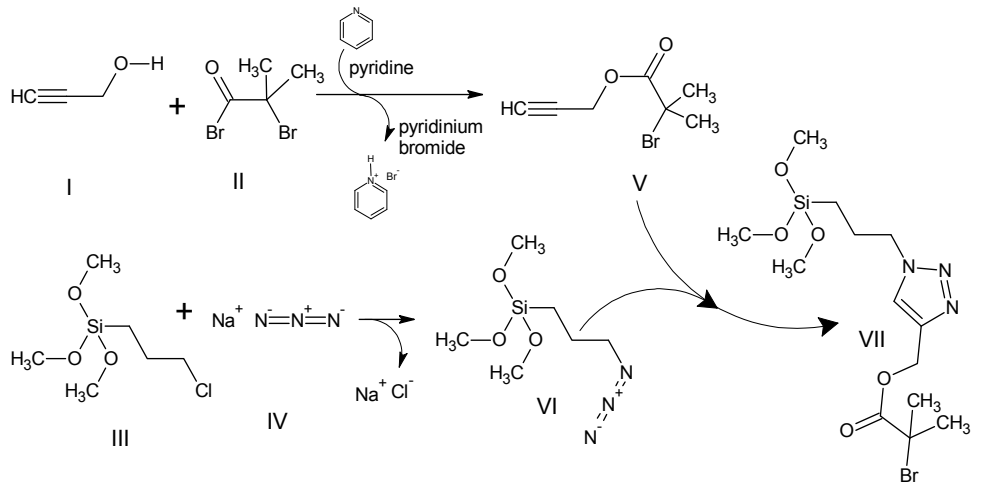

Scheme 1. Synthetic route to ATRP initiator silane coupling agent by "click" chemistry.

The decoration of Si-NPs (diameter 200 nm) was carried out in THF in the presence of a defined amount of the initiator-functional coupling agent. Prior to the reaction the Si-NPs were activated under acidic conditions to maximize the amount of active silanol groups of the surface followed by rigorous drying [37]. Evidence for a successful process was obtained from TGA (Figure 1) by a mass increase of 3.5%.

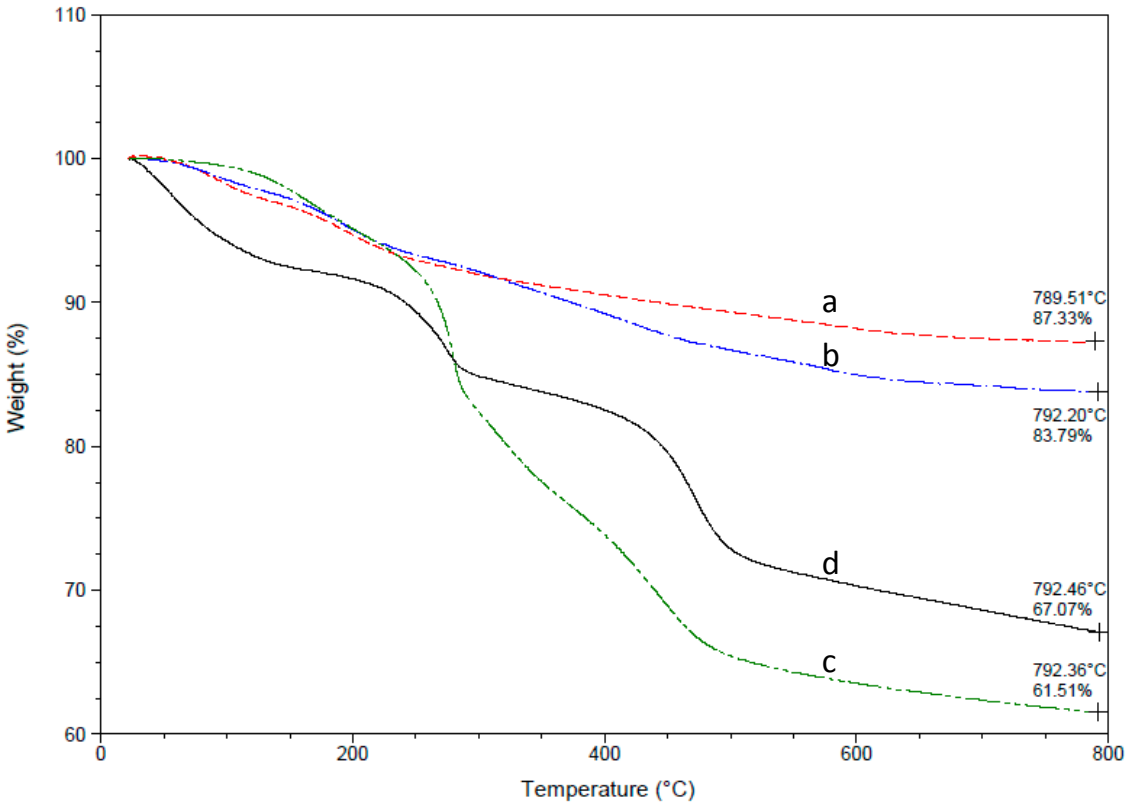

Figure 1. Thermo-gravimetric analysis (TGA) results of silica nano-particles (Si-NP) (diameter 200 nm) at various stages of decoration: (**a**) bare Si-NP; (**b**) initiator decorated Si-NP; (**c**) brush poly(*t*-BMA) decorated Si-NP (polymerization time 180 min.); (**d**) brush poly(methacrylic acid) (PMAA) decorated Si-NP. Note that all samples have been processed under the same conditions (freeze/drying for 5 days at 0.1 mPa at room temperature).

ARGET ATRP of *t*-BMA was then performed from the surface initiator decorated Si-NP using $CuCl_2$ and tris-((2-pyridyl)-methyl)-amine (TPMA) as the catalytic system, and tin(II)-2-ethylhexanoate as the reducing agent [24]. While it has been shown that direct ATRP of sodium methacrylate is possible from surfaces [38], it was decided to employ the protected monomer as that would avoid using an aqueous medium and potential hydrolysis of the particles under the reaction conditions. The polymerizations were carried out in the presence of a defined amount of free sacrificial initiator (methyl-2-bromopropionate) to mediate the reaction kinetics as well as the molecular weight of the polymer brushes [35]. A known amount of dimethylformamide (DMF) was added to the reaction system as an internal NMR standard. The ratio of the ^{1}H NMR signal intensity from the DMF methyl groups and the ^{1}H NMR signal intensity of the *tert*-butyl groups of the *t*-BMA monomer provide a measure of the consumed monomer during the polymerization. Fixed aliquots of the reaction mixtures were withdrawn at time intervals of 30 min using N_2 purged syringes. The collected samples were immediately exposed to air and cooled to stop the polymerization. After centrifugation the supernatant was analyzed by ^{1}H NMR to determine monomer conversion and by gel permeation chromatograms (GPC) to measure the molecular weight of the free polymer. The decanted Si-NPs were subsequently treated with HF to de-graft the polymer brushes and analyzed by GPC after precipitation in water/methanol to determine molecular weight and polydispersity.

It was found that the polymerization follows expected first order kinetics (Figure S2). More interesting is the comparison between the degrafted and the free PBMA. In Figure 2, the normalized GPC of the de-grafted polymers for the collected samples are presented. A clear shift of the chromatograms from low to high molecular weights can be seen. It is noticeable, however, that with increasing reaction time (monomer conversion) the low molecular weight tail of the traces hardly shifts, which is also manifested in an increasing polydispersity of the samples (Figure 3). This was not observed for the free polymer samples. Figure 3 shows a comparison of the molecular weights of the degrafted and free polymer. The very good agreement between both polymer molecular weights up to a monomer conversion of about 55% suggests that the growth conditions are nearly identical for the free and the surface grafted polymer. Moreover, the increase of M_n with monomer conversion is nearly linear in the 35%–55% monomer conversion range as would be expected for a controlled polymerization. At conversions of 75%, the measured M_n of the surface grafted polymer (156,000 g/mol) is significantly higher than that of the free polymers (55,000 g/mol). The deviation from the linearity for the surface polymerization suggests that the requirements for a controlled polymerization are not met anymore and uncontrolled growths occurs. As this is not the case for the free polymer, this must be caused by the specific confined surface conditions. It can be speculated that polymer end-groups are not assessable anymore for the catalytic system thus disturbing the delicate balance between dormant and active species resulting in uncontrolled radical polymerization. This is supported by a significant increase in the polydispersity of the de-grafted polymers from 1.3 to 3.5 at 75% monomer conversion (Figure 3). The assumption that free and grafted polymer populations are growing under the same conditions and produce polymers of comparable molecular weight and polydispersity is indeed not generally valid and in practice the comparability is strictly dependent on the specific condition used as the shape of the surface (flat or curved), the presence of confined pores or channels, the density of the grafted chains and the brush thickness can reverse this trend [39–44].

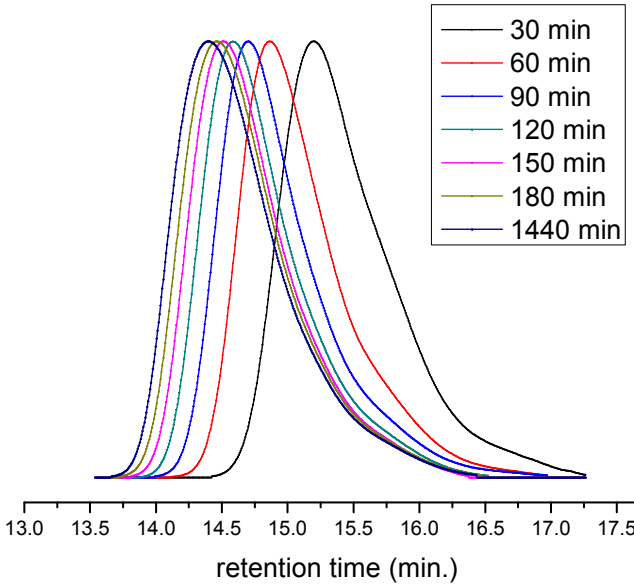

Figure 2. Gel permeation chromatograms (GPC) of the de-grafted polymers (normalized curves) at 30 min intervals and final sample after 24 h.

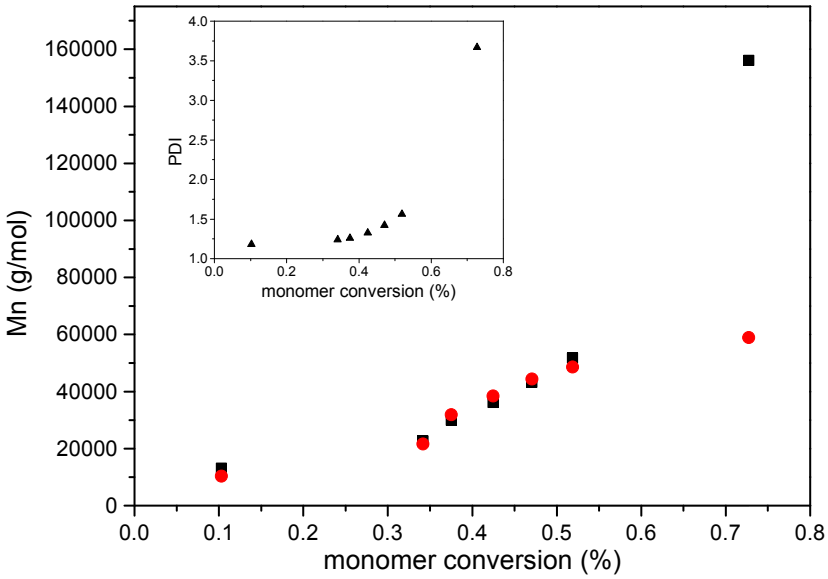

Figure 3. Molecular weights (M_n) and polydispersity (PDI, inset, ▲) of de-grafted polymer (■) and free polymer (●) as a function of monomer conversion.

TGA analysis (Figure 2) revealed a total polymeric brush mass of 17.9% for the PBMA decorated Si-NPs at 75% monomer conversion. Following the successful grafting of the PBMA brush, the final step was the deprotection of the *tert*-butyl groups to yield PMAA decorated Si-NP. Numerous methods have been reported for the deprotection of *tert*-butyl esters, although most involve the use of strong acids such as CF_3COOH, HCl, H_2SO_4, TsOH and MsOH or Lewis acids such as $BF_3{\cdot}OEt_2$, TMSI, TMSOTf, $TiCl_4$, $SnCl_4$, $AlCl_3$, $Sn(OTf)_2$, and $ZnBr_2$ [45,46]. However, strong acidic conditions and prolonged reaction times can promote hydrolytic reactions able to degraft the polymer chains from the Si-NP surface. Alternatively, the deprotection can also be achieved under mild acidic conditions by Montmorillonite K10 clay catalyst or silica gel (low pressure) but this approach would require separating NPs from

another solid phase [47]. Alternatively we investigated aqueous phosphoric acid (85 wt%) based on reports that it is an effective, environmentally benign reagent for the de-protection of *tert*-butyl carbamates, *tert*-butyl esters, and *tert*-butyl ethers [48,49]. The reaction conditions are mild, high yielding and offer good selectivity in the presence of other acid-sensitive groups such as cyclic carbamates, lactones, ketals, acetate esters. Figure 4 shows the attenuated total reflectance IR (ATR-IR) spectra of PBMA decorated Si-NP before and after treatment with aqueous phosphoric acid. Notably, the peaks characteristic of PBMA (Figure 4A) and PMAA (Figure 4B) can be identified and are in agreement with literature data [50,51]. For example, the C=O stretching (**1**) at 1720 cm^{-1} and peaks such as the broad peak at 1464 cm^{-1} (**2**, methyl group of the repeating unit), and the doublet at 1392 cm^{-1} and 1367 cm^{-1} (**3** and **4**), respectively, assigned to the *tert*-butyl group. After the deprotection step, peak **1** remains unchanged while the polymer main chain peak **2** can still be identified. Moreover, the presence of **3** and **4** suggest incomplete deprotection. Nevertheless, the nanoparticles were rendered hydrophilic as evident from their full dispersability in water as depicted in Figure 5. While the hydrophobic PBMA NP cannot be suspended in water, hydrophilic PMAA NP form a stable, homogeneous suspension within 5 s of ultra-sonication highlighting the change of hydrophilicity due to the deprotection process.

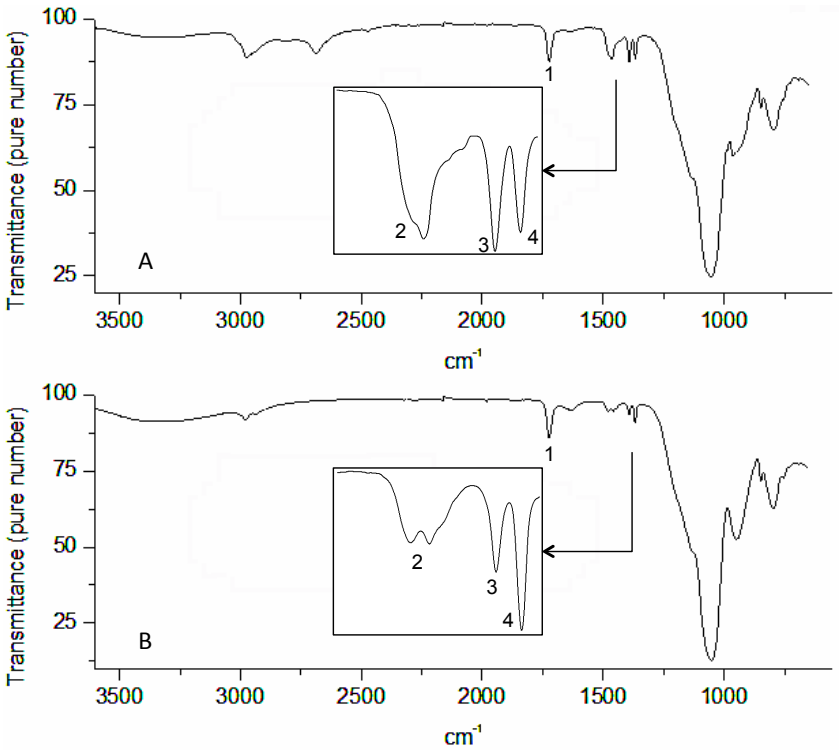

Figure 4. Attenuated total reflectance IR (ATR-IR) spectra of PBMA decorated Si-NP before (**A**) and after de-protection (**B**) with aqueous phosphoric acid.

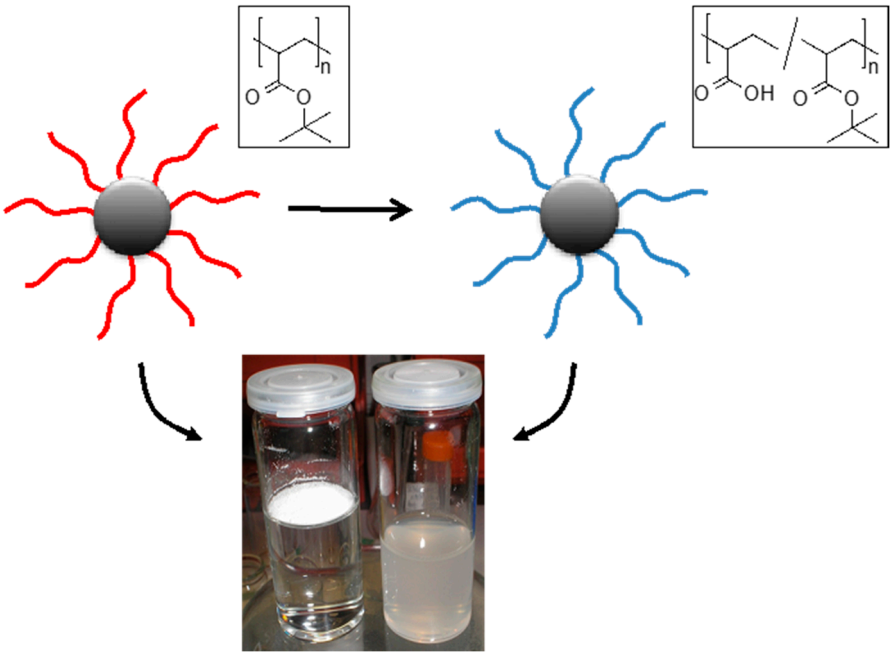

Figure 5. Hydrophobic PBMA decorated Si-NPs floating on water (left) and hydrophilic PMAA Si-NP suspended in water.

The deprotection yield for the PMAA Si-NP obtained at 75% monomer conversion was calculated from TGA analysis (Figure 1). A mass loss of 4.4% compared to the PBMA NP was measured after the deprotection step. Considering a theoretical weight loss of 8.6% at quantitative deprotection for this specific sample this corresponds to about 50% deprotection yield after 12 h of deprotection reaction (details on calculation see Supporting Information). It was found that this is indeed the maximal possible de-protection degree as prolonged reaction times result in undesired brush and NP hydrolysis (Figure S3). The incomplete deprotection is most likely due to a low accessibility of *t*-BMA groups close to the silica surface. It is here worthwhile to note, that this is not a negative feature as a hydrophobic region close to the nano-particles surface provides a protective barrier against hydrolysis of the polymeric chains. This is highlighted by the fact that treating the Si-NP suspensions at pH range 2–10 had no detectable detrimental effect on the suspension stability or particle quality (Figure S4). Moreover, this diffusion barrier is contributing to the stability of these monodisperse suspensions in 0.1 M phosphate buffer solution at pH 7.4 (monitored over one year), a pH of interest as the majority of proteins are stable under these conditions, which makes these nano-particles directly suitable for bio-conjugation.

Figure 6 depicts Field Emission Scanning Electron Microscopy (FE-SEM) image of Si-NP at different stages of decoration. In particular the brush decorated NP show a distinct core-shell structure (Figure 6D–F). The denser silica core appears as a dark gray (or blue in bright field mode) and the surrounding corona made of less dense PMAA brush appears as lighter gray or blue. The silica core is highly spherical as evident from the sharp border in the micrograph and the brush thickness of the surrounding polymeric corona is highly regular. For the 200 nm NP a brush thickness of 40 nm can be estimated. Generally PBMA brush decorated Si-NP show a higher tendency to melting under a 30 kV electron beam and the corona shadow surrounding the nano-particles in this case has a less sharply defined contour if compared to the de-protected system.

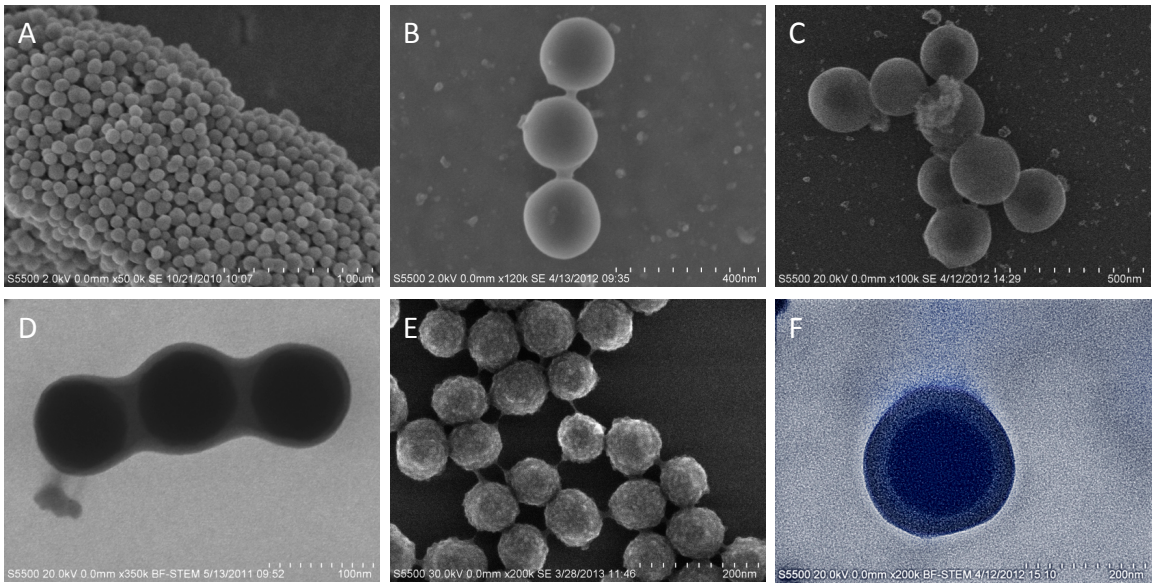

Figure 6. FE-SEM images of Si-NP of different size and state of decoration. (**A**) and (**B**): bare Si-NP; (**C**): ATRP initiator decorated NP; (**D**): PBMA brush decorated Si-NP; (**E**) and (**F**): PMAA brush decorated Si-NP.

Immobilization of biomolecules, such as proteins, enzymes, or antibodies on solid substrates has great importance in biosensors and biotechnology applications owing to their specific affinity for their targets [52,53]. Due to their robustness and versatility, functional polymer brushes have been utilized extensively for the immobilization of biomolecules [12,20,52–56]. Herein, horseradish peroxidase (HRP) has been chosen to conceptually investigate the covalent immobilization through carboxylic acid groups of PMAA decorated Si-NP. HRP is an α-helical globular protein with an average diameter of ~4.5 nm [50,57]. It is used extensively in biochemistry applications primarily for its ability to amplify a weak signal and increase detectability of a target molecule [58]. HRP immobilisation was performed using common EDC/sulfo-NHS coupling chemistry between amino groups of lysine residue of HRP and carboxyl groups of grafted PMAA at pH 7.4. A series of experiments was carried out systematically varying the weight ratio of HRP to PMAA decorated Si-NPs from 30, 40, 50, 60 and 70 µg HRP solutions (1 mg/mL) to 1 mg of NP suspension. The NP were subsequently washed and recovered by centrifugation. The enzymatic activity of the immobilized HRP was monitored using *o*-phexylene diamine dihydrochloride (OPD) as a chromogenic substrate. Upon reaction with HRP in the presence of hydrogen peroxide the soluble product 2,3-diaminophenazine is formed, which can be quantified UV spectroscopically at ~441 nm. Figure 7 shows a linear dependence of the UV absorbance peak from the HPR immobilised on the NP. When compared to the UV signal obtained from the free HRP at a centration that corresponds to the highest concentration used in the immobilisation protocol, a relative activity of 93% was relised. Slight activity loss could be due to inactive HRP on the surface, non-quantitative immobilisation or slight mosses in the work-up procedure.

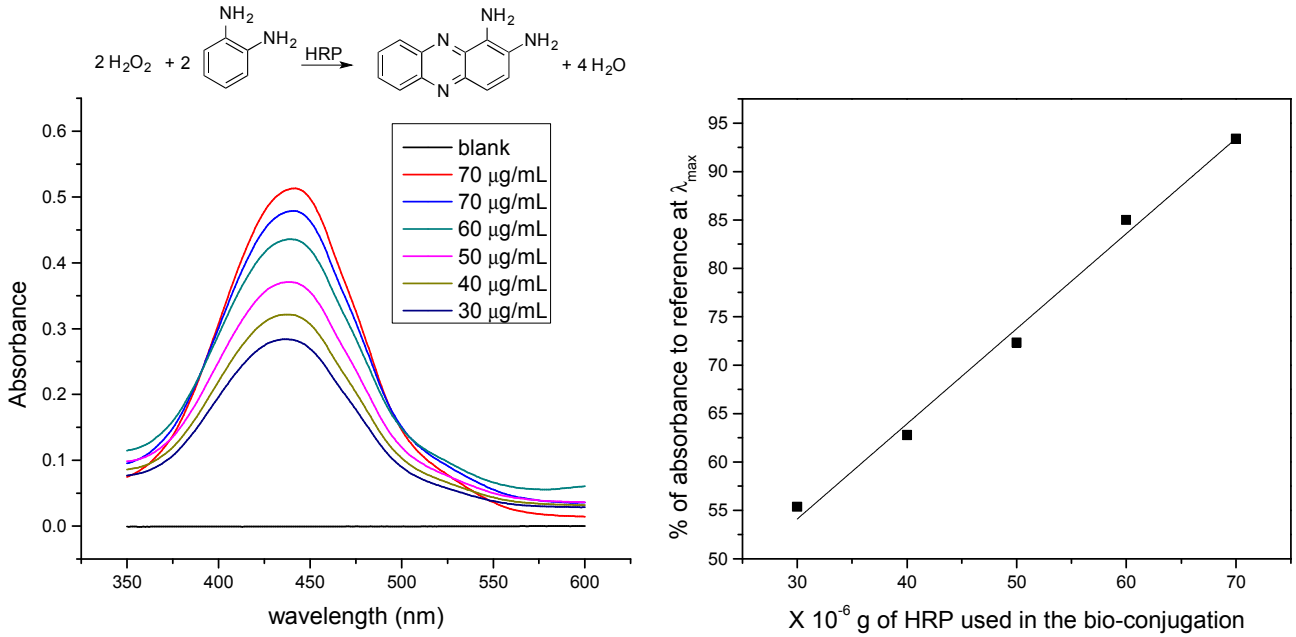

Figure 7. Horseradich peroxidase (HRP) catalysed conversion of *o*-phenylene diamine dihydrochloride (OPD) into 2,3-diaminophenazine and signficant UV-Vis absorbance peaks of 2,3-diaminophenazine for reactions catalysed by Si-NP conjugated with HRP at a concentration of 1 mg/mL NP in PBS at pH 7.4. Experiments 1–5 represent NP with decreasing amounts of conjugated HRP. The reference sample was recorded with free HRP (70 µg/mL), while the blank contains no HRP.

4. Conclusions

In conclusion, we have presented a robust protocol for the synthesis of PBMA polymer brushes on well-defined Si-NP using ARGET ATRP. The mild deprotection with phosphoric acid provided access to PMAA/PBMA copolymer brushes with high colloidal and pH stability. The feasibility for conjugation of active biomolecules to these particles was demonstrated by immobilization of HRP under retention of high level of catalytic activity.

Supplementary Materials

Supplementary materials can be accessed at: http://www.mdpi.com/2073-4360/7/8/1427.

Acknowledgments

This work was supported by funding from Science Foundation Ireland (07/IN1/B1792). Marcello Iacono gratefully acknowledges support from the Biomedical Diagnostic Institute (BDI) and the Irish Separation Science Cluster (ISSC).

Author Contributions

Marcello Iacono and Andreas Heise conceived and designed the experiments; Marcello Iacono performed the experiments; Marcello Iacono and Andreas Heise wrote the paper.

Conflicts of Interest

The authors declare no conflict of interest.

References

1. Jiang, T.; Mo, R.; Bellotti, A.; Zhou, J.; Gu, Z. Gel–liposome-mediated co-delivery of anticancer membrane-associated proteins and small-molecule drugs for enhanced therapeutic efficacy. *Adv. Funct. Mater.* **2014**, *24*, 2295–2304.
2. Hood, J.L.; Jallouck, A.P.; Campbell, N.; Ratner, L.; Wickline, S.A. Cytolytic nanoparticles attenuate HIV-1 infectivity. *Antivir. Ther.* **2013**, *18*, 95–103.
3. Thaxton, C.S.; Elghanian, E.; Thomas, A.D.; Stoeva, S.I.; Lee, J.-S.; Smith, N.D.; Schaeffer, A.J.; Klocker, H.; Horninger, W.; Bartsch, G.; *et al*. Nanoparticle-based bio-barcode assay redefines "undetectable" PSA and biochemical recurrence after radical prostatectomy. *Proc. Natl. Acad. Sci. USA* **2009**, *106*, 18437–18442.
4. Getts, D.R.; Martin, A.J.; McCarthy, D.P.; Terry, R.L.; Hunter, Z.N.; Yap, W.T.; Getts, M.T.; Pleiss, M.; Luo, X.R.; King, N.J.C.; *et al.* Microparticles bearing encephalitogenic peptides induce t-cell tolerance and ameliorate experimental autoimmune encephalomyelitis. *Nat. Biotechnol.* **2012**, *30*, 1217–1224.
5. Li, Y.; Chen, Y.; Xiang, R.; Ciuparu, D.; Pfefferle, L.D.; Horwath, C.; Wilkins, J.A. Incorporation of single-wall carbon nanotubes into an organic polymer monolithic stationary phase for μ-HPLC and capillary electrochromatography. *Anal. Chem.* **2005**, *77*, 1398–1406.
6. Chambers, S.D.; Holcombe, T.W.; Svec, F.; Frechet, J.M.J. Porous polymer monoliths functionalized through copolymerization of a C60 fullerene-containing methacrylate monomer for highly efficient separations of small molecules. *Anal. Chem.* **2011**, *83*, 9478–9484.
7. Stöber, W.; Fink, A.; Bohn, E. Controlled growth of monodisperse silica spheres in the micron size range. *J. Colloid. Interface Sci.* **1968**, *26*, 62–69.
8. Nyffenegger, R.; Quellet, C.; Ricka, J. Synthesis of fluorescent, monodisperse, colloidal silica particles. *J. Colloid Interface Sci.* **1993**, *159*, 150–157.
9. Xu, J.Q.; Sun, L.; Li, J.; Liang, J.L.; Zhang, H.M.; Yang, W.S. FITC and $Ru(phen)_3^{2+}$ co-doped silica particles as visualized ratiometric ph indicator. *Nanoscale Res. Lett.* **2011**, *6*, doi:10.1186/1556-276X-6-561.
10. Bin, Z.; Brittain, W.J. Polymer brushes: Surface-immobilized macromolecules. *Prog. Polym. Sci.* **2000**, *25*, 677–710.
11. Edmondson, S.; Steve, E.; Osborne, V.L.; Huck, W.T.S. Polymer brushes via surface-initiated polymerizations. *Chem. Soc. Rev.* **2004**, *33*, 14–22.
12. Audouin, F.; Larragy, R.; Fox, M.; O'Connor, B.; Heise A. Protein immobilization onto poly(acrylic acid) functional macroporous polyhipe obtained by surface-initiated ARGET ATRP. *Biomacromolecules* **2012**, *13*, 3787–3794.
13. Li, Z.F.; Ruckenstein, E. Water-soluble poly(acrylic acid) grafted luminescent silicon nanoparticles and their use as fluorescent biological staining labels. *Nano Lett.* **2004**, *4*, 1463–1467.

14. Chunzhao, L.; Benicewicz, B.C. Synthesis of well-defined polymer brushes grafted onto silica nanoparticles via surface reversible addition-fragmentation chain transfer polymerization. *Macromolecules* **2005**, 38, 5929–5936.
15. Rajesh, R.; Brittain, W.J. Synthesis of high density polymer brushes on nanoparticles by combined RAFT polymerization and click chemistry. *Macromol. Rapid Commun.* **2008**, *29*, 1104–1110.
16. Bindushree, R.; Ranjan, R.; Brittain, W.J. Surface initiated polymerizations from silica nanoparticles. *Soft Matter* **2006**, *2*, 386–396.
17. Von Werne, T.; Patten, T.E. Preparation of structurally well-defined polymer-nanoparticle hybrids with controlled/living radical polymerizations. *J. Am. Chem. Soc.* **1999**, *121*, 7409–7410.
18. Li, D.J.; Sheng, X.; Zhao, B. Environmentally responsive "hairy" nanoparticles: Mixed homopolymer brushes on silica nanoparticles synthesized by living radical polymerization techniques. *J. Am. Chem. Soc.* **2005**, *127*, 6248–6256.
19. Perruchot, C.; Khan, M.A.; Kamitsi, A.; Armes, S.V.; von Werne, T.; Patten, T.E. Synthesis of well-defined, polymer-grafted silica particles by aqueous ATRP. *Langmuir* **2001**, *17*, 4479–4481.
20. Barbey, R.; Lavanant, L.; Paripovic, D.; Schüwer, N.; Sugnaux, C.; Tugulu, S.; Klok, H.-A. Polymer brushes via surface-initiated controlled radical polymerization: Synthesis, characterization, properties, and applications. *Chem. Rev.* **2009**, *109*, 5437–5527.
21. Ke, M.; Gao, H.; Matyjaszewski, K. Use of ascorbic acid as reducing agent for synthesis of well-defined polymers by ARGET ATRP. *Macromolecules* **2007**, *40*, 1789–1791.
22. Jakubowski, W.; Matyjaszewski, K. Activators regenerated by electron transfer for atom-transfer radical polymerization of (meth)acrylates and related block copolymers. *Angew. Chem. Int. Edit.* **2006**, *45*, 4482–4486.
23. Abreu, C.M.R.; Mendonca, P.V.; Serra, A.C.; Popov, A.V.; Matyjaszewski, K.; Guliashvili, T.; Coelho, J.F.J. Inorganic sulfites: Efficient reducing agents and supplemental activators for atom transfer radical polymerization. *ACS Macro. Lett.* **2012**, *1*, 1308–1311.
24. Matyjaszewski, K.; Dong, H.C.; Jakubowski, W.; Pietrasik, J.; Kusumo, A. Grafting from surfaces for "everyone": ARGET ATRP in the presence of air. *Langmuir* **2007**, *23*, 4528–4531.
25. Hansson, S.; Ostmark, E.; Carlmark, A.; Malmstrom, E. ARGET ATRP for versatile grafting of cellulose using various monomers. *ACS Appl. Mater. Inter.* **2009**, *1*, 2651–2659.
26. Jonsson, M.; Nystrom, D.; Nordin, O.; Malmstrom, E. Surface modification of thermally expandable microspheres by grafting poly(glycidyl methacrylate) using ARGET ATRP. *Eur. Polym. J.* **2009**, *45*, 2374–2382.
27. Wang, M.; Yuan, J.; Huang, X.B.; Cai, X.M.; Li, L.; Shen, J. Grafting of carboxybetaine brush onto cellulose membranes via surface-initiated ARGET-ATRP for improving blood compatibility. *Colloid Surf. B* **2013**, *103*, 52–58.
28. Ma, W.; Otsuka, H.; Takahara, A. Poly(methyl methacrylate) grafted imogolite nanotubes prepared through surface-initiated ARGET ATRP. *Chem. Commun.* **2011**, *47*, 5813–5815.
29. Cheesman, B.T.; Willott, J.D.; Webber, G.B.; Edmondson, S.; Wanless, E.J. Ph-responsive brush-modified silica hybrids synthesized by surface-initiated ARGET ATRP. *ACS Macro. Lett.* **2012**, *1*, 1161–1165.

30. Zhao, M.N.; Zhou, G.W.; Zhang, L.; Li, X.Y.; Li, T.D.; Liu, F.F. Fabrication and photoactivity of a tunable-void sio2-tio2 core-shell structure on modified sio2 nanospheres by grafting an amphiphilic diblock copolymer using ARGET ATRP. *Soft Matter* **2014**, *10*, 1110–1120.
31. Gujadhur, R.; Venkataraman, D.; Kintigh, J.T. Formation of aryl-nitrogen bonds using a soluble copper(I) catalyst. *Tetrahedron Lett.* **2001**, *42*, 4791–4793.
32. Patel, V.K.; Vishwakarma, N.K.; Mishra, A.K.; Biswas, C.S.; Maiti, P.; Ray, B. Synthesis of alkyne-terminated xanthate raft agents and their uses for the controlled radical polymerization of *n*-vinylpyrrolidone and the synthesis of its block copolymer using click chemistry. *J. Appl. Polym. Sci.* **2013**, *127*, 4305–4317.
33. Paoprasert, P.; Spalenka, J.W.; Peterson, D.L.; Ruther, R.E.; Hamers, R.J.; Evans, P.G.; Gopalan, P. Grafting of poly(3-hexylthiophene) brushes on oxides using click chemistry. *J. Mater. Chem.* **2010**, *20*, 2651–2658.
34. Kolb, H.C.; Finn, M.G.; Sharpless, K.B. Click chemistry: Diverse chemical function from a few good reactions. *Angew. Chem. Int. Ed*. **2001**, *40*, 2004–2021.
35. Evans, R.A. The rise of azide-alkyne 1,3-dipolar "click" cycloaddition and its application to polymer science and surface modification. *Aust. J. Chem.* **2007**, *60*, 384–395.
36. Pretsch, C.; Seibl, S. *Tables of Spectral Data for Structure Determination of Organic Compounds*, 2nd Ed.; Sringer-Verlag: Berlin/Heidelberg, Germany, 1989.
37. Zhuravlev, L.T. The surface chemistry of amorphous silica. Zhuravlev model. *Colloids Surf. A* **2000**, *173*, 1–38.
38. Tugulu, S.; Barbey, R.; Harms, M.; Fricke, M.; Volkmer, D.; Rossi, A.; Klok, H.A. Synthesis of poly(methacrylic acid) brushes via surface-initiated atom transfer radical polymerization of sodium methacrylate and their use as substrates for the mineralization of calcium carbonate. *Macromolecules* **2007**, *40*, 168–177.
39. Turgman-Cohen, S.; Genzer, J. Simultaneous bulk- and surface-initiated controlled radical polymerization from planar substrates. *J. Am. Chem. Soc.* **2011**, *133*, 17567–17569.
40. Gorman, C.B.; Petrie, R.J.; Genzer, J. Effect of substrate geometry on polymer molecular weight and polydispersity during surface-initiated polymerization. *Macromolecules* **2008**, *41*, 4856–4865.
41. Koylu, D.; Carter, K.R. Stimuli-responsive surfaces utilizing cleavable polymer brush layers. *Macromolecules* **2009**, *42*, 8655–8660.
42. Devaux, C.; Chapela, J.P.; Beyou, E.; Chaumont, Ph. Controlled structure and density of "living" polystyrene brushes on flat silica surfaces. *Eur. Phys. J.* **2002**, *7*, 345–352.
43. Husseman, M.; Malmström, E.E.; McNamara, M.; Mate, M.; Mecerreyes, D.; Benoit, D.G.; Hedrick, J.L.; Mansky, P.; Huang, E.; Russell, T.P.; *et al.* Controlled synthesis of polymer brushes by "living" free radical polymerization techniques. *Macromolecules* **1999**, *32*, 1424–1431.
44. Pasetto, P.; Blas, H.; Audouin, F.; Boissiere, C.; Sanchez, C.; Save, M.; Charleux, B. Mechanistic insight into surface-initiated polymerization of methyl methacrylate and styrene via ATRP from ordered mesoporous silica particles. *Macromolecules* **2009**, *42*, 5983–5995.
45. Bose, D.S.; Kumar, K.K.; Reddy, A.V.N. A new protocol for selective deprotection of *N*-*tert*-butoxycarbonyl protective group (*t*-Boc) with $Sn(OTf)_2$. *Synth. Commun.* **2003**, *33*, 445–450.
46. Greene, T.W.; Wuts, P.G.M. *Protective Groups in Organic Synthesis*, 3rd ed.; John Wiley & Sons Inc.: New York, NY, USA, 1999.

47. Apelqvist, T.; Wensbo, D. Selective removal of the *N*-BOC protective group using silica gel at low pressure. *Tetrahedron Lett.* **1996**, *37*, 1471–1472.
48. Li, B.; Berliner, M.; Buzon, R.; Chiu, C.K.F.; Colgan, S.T.; Kaneko, T.; Keene, N.; Kissel, W.; Le, T.; Leeman, K.R.; *et al.* Aqueous phosphoric acid as a mild reagent for deprotection of *tert*-butyl carbamates, esters, and ethers. *J. Org. Chem.* **2006**, *71*, 9045–9050.
49. Li, B.; Bemish, R.; Buzon, R.A.; Chiu, C.K.F.; Colgan, S.T.; Kissel, W.; Le, T.; Leeman, K.R.; Newell, L.; Roth, J. Aqueous phosphoric acid as a mild reagent for deprotection of the *t*-butoxycarbonyl group. *Tetrahedron Lett.* **2003**, *44*, 8113–8115.
50. Shin, H.S.; Jung, Y.M.; Chang, T.; Ozaki, Y.; Kim, S.B. Characterization of β-transition of poly(*tert*-butyl methacrylate) thin films by two-dimensional infrared correlation spectral analysis. *Vib. Spectrosc.* **2002**, *29*, 73–77.
51. Metaxa, A.F.; Efthimiadou, E.K.; Boukos, N.; Kordas, G. Polysaccharides as a source of advanced materials: Cellulose hollow microspheres for drug delivery in cancer therapy. *J. Colloid Interface Sci.* **2012**, *384*, 198–206.
52. Jiang, H.; Xu, F.J. Biomolecule-functionalized polymer brushes. *Chem. Soc. Rev.* **2013**, *42*, 3394–3426.
53. Goddard, J.M.; Hotchkiss, J.H. Polymer surface modification for the attachment of bioactive compounds. *Prog. Polym. Sci.* **2007**, *32*, 698–725.
54. Ates, Z.; Audouin, F.; Harrington, A.; O'Connor, B.; Heise, A. Functional brush-decorated poly(globalide) films by ARGET-ATRP for bioconjugation. *Macromol. Biosci.* **2014**, *14*, 1600–1608.
55. Audouin, F.; Fox, M.; Larragy, R.; Clarke, P.; Huang, J.; O'Connor, B.; Heise, A. Polypeptide-grafted macroporous polyhipe by surface-initiated n-carboxyanhydride (NCA) polymerization as a platform for bioconjugation. *Macromolecules* **2012**, *45*, 6127–6135.
56. Xu, F.J.; Neoh, K.G.; Kang, E.T. Bioactive surfaces and biomaterials via atom transfer radical polymerization. *Prog. Polym. Sci.* **2009**, *34*, 719–761.
57. Erickson, H.P. Size and shape of protein molecules at the nanometer level determined by sedimentation, gel filtration, and electron microscopy. *Biol. Proced. Online.* **2009**, *11*, 32–51.
58. Yang, S.; Jia, W.Z.; Qian, Q.Y.; Zhou, Y.G.; Xia, X.H. Simple approach for efficient encapsulation of enzyme in silica matrix with retained bioactivity. *Anal. Chem.* **2009**, *81*, 3478–3484.